

Act, Think or Abstain: Complexity-Aware Adaptive Inference for Vision-Language-Action Models

Riccardo Andrea Izzo[†], Gianluca Bardaro[†], and Matteo Matteucci[†]

Abstract—Current research on Vision-Language-Action (VLA) models predominantly focuses on enhancing generalization through established reasoning techniques. While effective, these improvements invariably increase computational complexity and inference latency. Furthermore, these mechanisms are typically applied indiscriminately, resulting in the inefficient allocation of resources for trivial tasks while simultaneously failing to provide the uncertainty estimation necessary to prevent catastrophic failure on out-of-distribution tasks. Inspired by human cognition, we propose an adaptive framework that dynamically routes VLA execution based on the complexity of the perceived state. Our approach transforms the VLA’s vision-language backbone into an active detection tool by projecting latent embeddings into an ensemble of parametric and non-parametric estimators. This allows the system to execute known tasks immediately (*Act*), reason about ambiguous scenarios (*Think*), and preemptively halt execution when encountering significant physical or semantic anomalies (*Abstain*). In our empirical analysis, we observe a phenomenon where visual embeddings alone are superior for inferring task complexity due to the semantic invariance of language. Evaluated on the LIBERO and LIBERO-PRO benchmarks as well as on a real robot, our vision-only configuration achieves 80% F1-Score using as little as 5% of training data, establishing itself as a reliable and efficient task complexity detector.

I. INTRODUCTION

A unique trait of human intelligence is the ability to dynamically calibrate cognitive effort based on task demands. For routine tasks, we rely on fast and reactive decision-making, while for novel and ambiguous scenarios, we inherently analyze and reason about the task. When faced with a completely new task that goes beyond our abilities, we instinctively abstain to avoid damage. Nowadays, one promising direction for enhancing generalisation and adaptability in robotics is the use of Vision-Language-Action (VLA) models, end-to-end policies capable of grounding language and vision in the physical world. Despite their impressive capabilities, current VLAs lack this adaptive flexibility. Prior works have explored augmenting these with intermediate reasoning steps, such as Chain-of-Thought (CoT), significantly improving performance [1]–[3]. While effective, this push towards embodied reasoning comes at the non-negligible cost of increased computational complexity and inference latency, regardless of task difficulty. This results in the inefficient resource allocation for trivial tasks, and more critically, a failure to recognize when a task is completely out-of-distribution, leading to overconfident but catastrophic execution. In this paper, we advocate for a transition toward

complexity-aware VLAs. We argue that a truly generalist policy should not act immediately, but consider the difficulty of the task before executing. We thus propose a framework that dynamically orchestrates VLA execution based on the complexity of the perceived state. Our approach leverages the VLA’s pre-trained VLM backbone, transforming it from a passive feature extractor in latent space to an active complexity detector. This allows the system to execute known tasks with minimal latency overhead (*Act*), perform additional reasoning when the environment or the task is ambiguous (*Think*), or preemptively halt the execution when encountering heavy semantic or physical anomalies (*Abstain*). Our pipeline leverages the extracted embeddings and scores them using an ensemble of parametric Gaussian Mixture Models (GMMs) and non-parametric k-Nearest Neighbour (kNN). These scores are processed by a simple MLP to map the distribution of vision, text, and fused features to the optimal execution strategy. Notably, our method is agnostic to both VLMs and different types of VLA architectures, and hence can be applied to diverse control policies. Our ablation studies demonstrate that visual embeddings alone provide the most reliable signals for inferring task complexity. In contrast, the semantic invariance of language features tends to mask subtle execution anomalies. These results confirm recent findings on the predominant role of vision in VLAs: while vision-language fusion is the standard for action policy generation, it can be significantly detrimental for assessing physical task complexity [4]. By employing the visual embeddings exclusively, our GMM configuration achieves an 80% F1-Score in identifying partially OOD tasks, while maintaining high efficiency with only 5% of training data required. Our key contributions include:

- A novel framework to infer task complexity using embeddings extracted from the VLM backbone of a VLA.
- An adaptive system (i.e., Act, Think, or Abstain) that resolves the implicit trade-off between improved generalization, real-time responsiveness, and intentional safety.
- A detailed analysis of the different modalities extracted from VLAs, demonstrating that visual representations are superior to fused representations for physical safety.
- An extensive evaluation in simulation (LIBERO and LIBERO-PRO benchmarks) as well as on a real robot (SO-ARM 101), showing robust performance using as little as 5% of the available training data.

By enabling VLAs to recognize the limits of their own capabilities, our framework provides a critical step toward

[†]All authors are with the Department of Electronics, Information, and Bioengineering, Politecnico di Milano, Milan, Italy. E-mail: name.surname@polimi.it

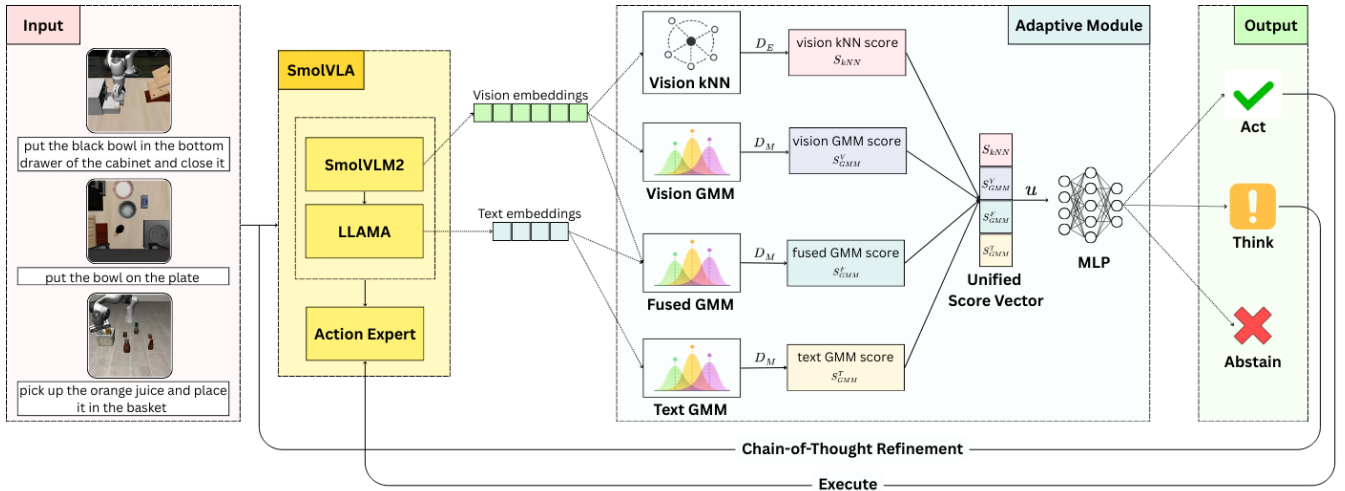


Fig. 1. **Overview of our framework.** Given an image observation and a language instruction of a task, the system extracts text and vision embeddings from the SmolVLA backbone. These embeddings are scored using an ensemble of GMMs and kNN. The resulting scores are consolidated into a unified score vector and processed by a custom MLP to select the optimal execution strategy. High confidence triggers direct execution (*Act*), while ambiguous scenarios result in additional reasoning (*Think*). Tasks which are entirely out-of-distribution invoke a safety fallback and prevent execution (*Abstain*).

deploying foundation models in safety-critical and open-ended robotic environments. We release code and models¹.

II. RELATED WORKS

A. Vision-Language-Action Models

Recent advancements in robot learning have increasingly relied on Vision-Language-Action (VLA) models, end-to-end systems that unify perception and natural language to directly generate robot actions. Building upon the foundations of Large Language Models (LLMs) and Vision-Language Models (VLMs), VLAs are typically trained on massive multimodal datasets comprising text, vision, and robot trajectories [5], [6]. Early works, such as RT-2 [7] and OpenVLA [8], adapted standard VLMs to output actions as discretized text tokens via autoregressive decoding. However, to overcome the precision limitations of discretization, subsequent research has pivoted toward continuous action generation. Notably, models like π_0 integrate flow-matching networks directly into the architecture to produce high-frequency continuous robot trajectories [9]. While some models are monolithic, other works advocate for modular architectures that decouple high-level reasoning from low-level control, such as GROOT [10], which employs a dual-system design to balance reasoning with real-time execution. Furthermore, to refine accuracy, recent methods have incorporated reinforcement learning policies during the fine-tuning stage, utilizing reward feedback to correct prediction errors and improve robustness [11], [12]. Finally, addressing the computational constraints of deployment on a real robot, recent efforts have focused on efficiency by developing VLAs based on compact backbones, such as SmolVLA and TinyVLA, while retaining competitive performance with significantly lower resource requirements [13], [14].

B. Embodied Reasoning in VLAs

Building upon standard VLA architectures, recent models have explored enhancing direct action prediction with intermediate reasoning steps. Approaches such as Embodied Chain-of-Thought (ECoT) [1], CoT-VLA [2], and InstructVLA [15] generate additional reasoning traces, sub-goals, or scene descriptions before execution, significantly improving overall success rates. Similarly, hierarchical frameworks like Steerable Policies [16] leverage a high-level VLM reasoner to dynamically issue steering commands, ranging from subtasks to grounded pixel coordinates. While works like Fast ECoT [3] make efforts to reduce the latency of these additional generation steps, running massive reasoning models at control frequencies remains a computational bottleneck. Furthermore, these methods typically enforce reasoning at every timestep, which is inefficient for trivial tasks. Current works such as OneTwoVLA [17] and SAFE [18] have started mitigating these issues by adaptively restricting explicit reasoning to critical moments or by analyzing feature spaces to detect execution failures. In contrast, our framework treats reasoning as a conditional fallback. By evaluating the complexity of the latent representation, our pipeline directly executes known tasks and reserves heavy reasoning steps exclusively for unfamiliar or complex scenarios. At the same time, for tasks that exceed the model’s capabilities, our pipeline can predict failure, thus avoiding unnecessary reasoning and consequent catastrophic execution errors.

III. METHOD

Our approach leverages SmolVLA [13] as the reference Vision-Language-Action architecture, which integrates a pre-trained SmolVLM-2 [19] backbone with an action expert optimized via flow-matching [20]. To enable the agent to be aware of task complexity and act accordingly, we propose a pipeline that transforms the embeddings extracted from the VLM into a routing mechanism for adaptive inference. In

¹<https://github.com/AIRLab-POLIMI/ActThinkAbstain>

Section III-A, we define the extraction and preprocessing of multimodal features from the VLM backbone. We then describe in Section III-B our strategy to model the In-Distribution (ID) manifold using both parametric and non-parametric methods to quantify feature novelty. Section III-C illustrates how these scores are unified into a single vector and mapped to the discrete set of strategies (i.e., Act, Think, Abstain). Finally, Section III-D outlines the training procedure for our pipeline.

A. Feature Extraction Pipeline

We begin by extracting unimodal and multimodal features at inference time from the VLM backbone to capture linguistic ambiguity, visual novelty and vision-language misalignment. Given a batch of image observations and language instructions, the images are processed by the ViT encoder (16×16 patches, 12 transformer layers), while language tokens are processed in parallel by the LLaMA [21] text decoder. Notably, we isolate the two modalities from each other by forwarding language tokens without visual conditioning. This ensures that the text embeddings reflect only linguistic uncertainty rather than grounded scene information. Let B denote the batch size, N_c the number of camera views, and S_v, S_t the sequence lengths for visual and text inputs respectively. The feature dimensions are $D_v = 768$ for the vision encoder and $D_t = 960$ for the text decoder. The feature extraction is defined as follows:

Visual Features (\mathbf{z}_{vis}): Extracted from the last hidden states of the ViT encoder. To capture high-level semantic scene novelty before LLM projection, we perform spatial average pooling across the S_v patches per camera, followed by mean pooling across all N_c views to obtain $\mathbf{z}_{\text{vis}} \in \mathbb{R}^{B \times D_v}$.

Text Features (\mathbf{z}_{text}): Extracted from the LLaMA decoder’s last hidden layer. We forward the language tokens without visual conditioning, treating the model as a pure text encoder. We apply masked mean pooling across the sequence S_t , obtaining $\mathbf{z}_{\text{text}} \in \mathbb{R}^{B \times D_t}$.

Fused Features ($\mathbf{z}_{\text{fused}}$): To quantify vision-language mismatch, we implement a late fusion strategy. Both \mathbf{z}_{vis} and \mathbf{z}_{text} are normalized with L_2 and concatenated to form a joint representation $\mathbf{z}_{\text{fused}} = [\bar{\mathbf{z}}_{\text{vis}} \parallel \bar{\mathbf{z}}_{\text{text}}] \in \mathbb{R}^{B \times (D_v + D_t)}$.

B. Distribution Fitting and OOD Scoring

Direct density estimation on the feature vectors \mathbf{z} is often computationally expensive due to the curse of dimensionality. To mitigate this, we first apply Principal Component Analysis (PCA) to project the features into a lower-dimensional space $D' = 64$, preserving 95% of the maximum variance and filtering out noise. The resulting reduced features, denoted as \mathbf{z}' , serve as input for our scoring modules.

Gaussian Mixture Model (GMM): To account for the multimodal nature of robotic task clusters, we model the training distribution of the latent features as a GMM with K components [22]. To quantify the novelty of a sample \mathbf{z}' , we compute the Mahalanobis distance [23] to each Gaussian component k in the mixture:

$$D_M(\mathbf{z}', \mu_k, \Sigma_k) = \sqrt{(\mathbf{z}' - \mu_k)^\top \Sigma_k^{-1} (\mathbf{z}' - \mu_k)} \quad (1)$$

where μ_k and Σ_k are the sample mean and the covariance of the k -th component. However, when the feature dimensionality D' approaches or exceeds the sample size N in scenarios with scarce data, the covariance matrix Σ_k may become singular or ill-conditioned. To ensure that the matrix is invertible for Mahalanobis distance calculations, we employ the Ledoit-Wolf shrinkage estimator [24]:

$$\Sigma_{LW} = (1 - \rho) \Sigma_{emp} + \rho \frac{\text{Tr}(\Sigma_{emp})}{D'} \mathbf{I} \quad (2)$$

where $\text{Tr}(\cdot)$ denotes the trace operator and $\rho \in [0, 1]$ is the shrinkage coefficient (default $\rho = 0.01$). This parametric formulation effectively handles complex task distributions but incurs a higher computational cost. We finally define the GMM score, S_{GMM} , as the Mahalanobis distance D_M to the closest Gaussian component k :

$$S_{GMM}(\mathbf{z}') = \min_k D_M(\mathbf{z}', \mu_k, \Sigma_k) \quad (3)$$

k-Nearest Neighbours (kNN): As a non-parametric alternative, we compute local density without assuming a global distribution. The kNN score is defined as the Euclidean distance to the nearest neighbour in the training set X_{train} :

$$D_E(\mathbf{z}', \mathbf{x}'_i) = \|\mathbf{z}' - \mathbf{x}'_i\|_2 \quad (4)$$

$$S_{kNN}(\mathbf{z}') = \min_{\mathbf{x}'_i \in X'_{\text{train}}} D_E(\mathbf{z}', \mathbf{x}'_i) \quad (5)$$

We specifically utilize 1-NN to maximize sensitivity to subtle anomalies, ensuring that isolated and uncommon states remain clearly detectable rather than being smoothed out by neighbour averaging. By utilizing both parametric (i.e., GMM) and non-parametric (i.e., kNN) estimators, we capture both global structure and local geometric density. While kNN provides local sensitivity to outliers, GMMs result in a probabilistic estimator that can handle complex task distributions, ideal for robotics. Together, they allow the system to reliably detect both localized execution anomalies and broad distribution shifts in open-ended environments.

C. Score Aggregation

The scores derived from visual, text, and fused representations provide a detailed view of uncertainty regarding the task complexity. However, as the magnitude and the ranges of these scores are intrinsically linked to the statistical variance of the in-distribution training set, a direct approach based on thresholds is insufficient for effective decision making. We therefore propose to learn a function that maps these scores to a discrete system strategy. We first consolidate these scores into a unified vector $\mathbf{u} \in \mathbb{R}^4$:

$$\mathbf{u} = [S_{GMM}^V, S_{GMM}^L, S_{GMM}^F, S_{kNN}]^\top \quad (6)$$

Notably, for the kNN estimator, we exclusively utilize visual features. We observe that text features in the training set exhibit high structural redundancy (e.g., repetitive task instructions), which collapses the local density in kNN, leading to extreme sensitivity to minor variations. Similarly, while GMMs provide a more flexible option, they remain susceptible to overfitting when text clusters are highly

discrete. We quantify the impact of these text features in Section IV-C. Given the non-linear relationship between the computed scores and the actual success on the robot, we employ a Multi-Layer Perceptron (MLP) to predict the optimal execution strategy. The vector \mathbf{u} is processed through Batch Normalization (BN) followed by a hidden layer with a ReLU activation σ :

$$\mathbf{y} = \text{softmax}(W_2 \cdot \sigma(W_1 \cdot \text{BN}(\mathbf{u}) + b_1) + b_2) \quad (7)$$

where \mathbf{y} is the probability distribution over three distinct operational states. The final system policy is determined as the *argmax* of the output vector \mathbf{y} :

$$\text{Action} = \begin{cases} \text{Act (ID)} & \text{if } \text{argmax}(\mathbf{y}) = 0 \\ \text{Think (Partially OOD)} & \text{if } \text{argmax}(\mathbf{y}) = 1 \\ \text{Abstain (OOD)} & \text{if } \text{argmax}(\mathbf{y}) = 2 \end{cases} \quad (8)$$

The MLP maps the scores to one of three strategic outcomes, balancing efficiency and safety. In the *Act* option, the task is recognized to be within the training distribution with high confidence, and the robot proceeds with immediate execution using the base VLA policy. Conversely, if the system selects *Think*, it has detected a degree of semantic or visual ambiguity. This option pauses the execution to engage the VLM backbone in additional reasoning steps, aiming to resolve the mismatch before acting. The reasoning steps include extracting scene cues (e.g., object pose, object relations) as well as inferring subgoals from the current task instruction. These additional informations are appended to the input text prompt, effectively grounding the VLM before action generation. Notably, the "Think" branch happens once per episode during the first timestep. Finally, the *Abstain* option provides a critical fallback for tasks that lie completely outside the model’s capabilities. With this option, the task is dismissed to prevent a potential catastrophic failure.

D. Training

To ground our system, we selected *Hugging-FaceVLA/smolvla_libero*, which is pre-trained on LIBERO [25]. We define a suite of training datasets categorized by the three levels of distribution shift (i.e., ID, partially OOD, OOD). We consider the original LIBERO tasks to be in-distribution (ID), as the model has been fine-tuned on them, representing the baseline for the *Act* path. For partially OOD tasks related to the *Think* option, we employ LIBERO-PRO [26], which introduces five types of perturbations (i.e., object, position, semantic, task, and environment) that significantly hinder baseline VLA performance. Finally, for completely OOD tasks in the *Abstain* case, we collect trajectories from a tabletop manipulation dataset (i.e., *lerobot/nyu_franka_play_dataset*, *lerobot/cmu_franka_exploration_dataset*) featuring the same Franka Panda manipulator but under different scenarios (camera viewpoint, lighting, background, and object sets), making them outside the VLA capabilities. The full training corpus is then partitioned into a 50% split for detector fitting, 25% for MLP training, and 25% for validation.

Detector Calibration: As detailed in Section III-B, raw features are initially normalized and projected via PCA, preserving 95% of the variance. We parameterised the GMMs using five random starts to mitigate the risk of local minima. Concurrently, a kNN index ($k = 1$) is populated with the same projected features.

MLP Training: The MLP is trained to map the unified vector \mathbf{u} to the three states illustrated in Section III-C. We employ a lightweight architecture with two hidden layers of size 64 and 32, respectively. Training is conducted using a cross-entropy loss with a learning rate of 10^{-3} and early stopping on the validation set (i.e., 15% of the training split reserved to the MLP) to prevent overfitting. A key challenge in training the MLP relies on the partially OOD samples. While ID and OOD boundaries are often clear, there is a lack of standard benchmarks for this intermediate case, with the transition in real settings being continuous rather than discrete. In real deployments, we can usually obtain examples of ID tasks (e.g., the model’s training set) and identify clearly OOD scenarios, but we generally lack a curated set for partially OOD cases. Although benchmarks such as LIBERO-PRO can serve as partial OOD for our task, this assumption relies on having the corresponding LIBERO distribution as the ID reference and does not generalize across VLA models. Consequently, to simulate this transition, we employ a mixup strategy [27] using a Beta distribution, interpolating between ID and OOD distributions and generating synthetic intermediate features:

$$\mathbf{z}_{think} = \lambda \mathbf{z}_{ID} + (1 - \lambda) \mathbf{z}_{OOD}, \quad \lambda \sim \text{Beta}(0.5, 0.5) \quad (9)$$

This approach forces the MLP to learn a robust decision boundary for tasks that are neither fully known nor completely new, effectively supervising the model to trigger additional reasoning when direct execution confidence is compromised.

Baseline MLP Training: To quantify the efficacy of our system, we also train an MLP directly on the concatenated raw embeddings:

$$\mathbf{u} = [\mathbf{z}_{vis}, \mathbf{z}_{text}, \mathbf{z}_{fused}]^T \quad (10)$$

To ensure a fair comparison, the baseline utilizes the same mixup strategy and a comparable lightweight architecture with two hidden layers of size 512 and 128, batch normalization, and dropout. We maintain the same learning rate of 10^{-3} with early stopping on the identical validation set.

IV. EXPERIMENTAL RESULTS

In this section, we provide a comprehensive evaluation of our framework across a diverse set of robotic manipulation tasks. Our experiments are designed to validate the system’s ability to infer the task complexity at inference time and select an optimal execution strategy. We assess the performance of our pipeline using the LIBERO and LIBERO-PRO benchmarks, focusing on scenarios where standard VLAs typically struggle due to distribution shifts. Specifically, we aim to address the following research questions (RQ):

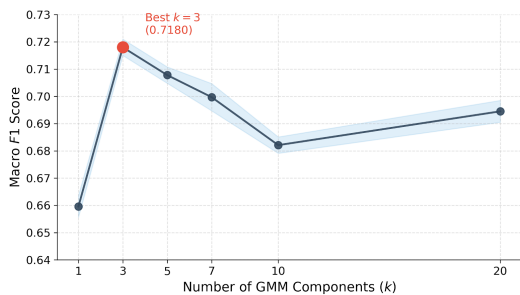


Fig. 2. **Impact of GMM components k on OOD detection.** The F1-score peaks at $k = 3$, demonstrating that while multiple Gaussians are necessary to capture the task manifold’s complexity, further increases lead to overfitting and diminishing returns. Variance remains stable across the tested range.

- **RQ1:** What are the individual contributions of GMM, kNN, and the MLP across different modalities in detecting task distribution shift?
- **RQ2:** To what extent does our scoring pipeline effectively divide the tasks into ID, partially OOD, and fully OOD clusters?
- **RQ3:** Does the learned policy significantly reduce catastrophic failures in OOD scenarios, while maintaining or improving the success rate in partially OOD ones?
- **RQ4:** What is the trade-off between the computational overhead of the ensemble (GMM + kNN + MLP) and the gains in overall system reliability?

A. GMM Component Count

A critical parameter in our pipeline is the number of Gaussian components k for the GMMs, which defines the granularity that the model uses to approximate the task distribution. Since the robotic domain involves diverse object interactions and environmental conditions, k must be sufficiently high to capture these shifts without overfitting to local noise. We conducted an ablation study by varying k and monitoring the resulting macro F1-score across a validation set balanced between ID and OOD tasks. As illustrated in Figure 2, the best performance is achieved at $k = 3$, with slightly diminishing returns as k increases. The significant performance drop at $k = 1$ highlights the limitations of a single Gaussian to model the complex robotic domain. Conversely, as k increases beyond three, we observe slightly diminishing returns and increased computational overhead.

B. Data Scaling

To quantify the amount of data required by our pipeline, we evaluate the framework across seven distinct configurations under an increasing number of data samples. The baseline MLP consists of concatenated raw features without uncertainty estimation. We compare this against unimodal variants (i.e., text-only, vision-only, and fused GMMs) as well as a KNN variant. Finally, we assess the ensemble configurations, comprising both GMMs and kNN. Concretely, we subsample the training set at $\{0.1\%, 1\%, 5\%, 10\%, 25\%\}$, going from 64 to 15,885 samples. Figure 3 reveals three key trends using the Macro F1-Score as the main metric.

First, the baseline MLP trained on raw features remains almost insensitive to the size of the dataset, yielding a stable but mediocre performance ($F1 \approx 0.60$) across all training fractions. This suggests that, without the density estimators, the model cannot effectively separate the manifold, even when additional data is available. Secondly, methods leveraging vision features exhibit the strongest scaling. While the vision-only GMM struggles with extremely low data (0.1%), it improves quickly, outperforming the baseline by 15% once just 1% (i.e., less than 1,000 samples) of the data is available. Performance converges around 5%, confirming that the pipeline can effectively learn even with scarce data, once the underlying distribution is stabilized. Finally, the multimodal GMM ensemble achieves the highest robustness at 0.1%. This indicates that, while additional modalities may introduce noise when dealing with large datasets, they provide a beneficial regularization effect when dealing with few samples, preventing the MLP from overfitting to sparse vision clusters. Concurrently, the non-parametric kNN degrades significantly at 0.1% due to local sample sensitivity, which becomes critically sparse with extremely low data. Overall, the pipeline demonstrates higher efficiency compared to the baseline MLP, reaching near-peak performance with as low as 5% of available training data, making it very suitable for robotics applications with limited labeled data.

C. Pipeline Effectiveness (RQ1, RQ2)

We evaluate all configurations from Section IV-B to isolate the contribution of every component using the full dataset. As evaluation metrics, we consider Precision, Recall, and Macro F1-Score. Results are summarized in Figure 3, while in Figure 4 we report the confusion matrices for each configuration.

Importance of Vision Modality: Our MLP + GMM (vision-only) configuration achieves the best results with a Macro F1-Score of 84.34%, outperforming every alternative by a significant margin. This indicates that the vision embeddings are the most reliable signal to infer decision boundaries across ID, partially OOD, and fully OOD tasks. The MLP + kNN on vision data remains competitive with an F1-Score of 73.90%, but its lower performance compared to GMM implies that a parametric density estimator better captures the complex structure of the vision manifold. Notably, it exhibits no confusion between the "Act" and the "Abstain" path, ensuring that the system never mistakenly executes a task that requires halting. It also demonstrates the highest sensitivity to the "Think" path, confirming it to be the most difficult class to distinguish across all models.

Baseline: The baseline MLP trained directly on raw features obtains a Macro F1-Score of 63.81%. While it correctly identifies the "Act" and "Abstain" with high accuracy, it results in being overconfident, as 86% of "Think" scenarios are misclassified as "Act". This confirms the difficulty of the model in consistently recognizing ambiguity, potentially leading to unsafe execution in robotic tasks.

Multimodal Interference: In our experiments, the inclusion of text and fused embeddings appears detrimental. While

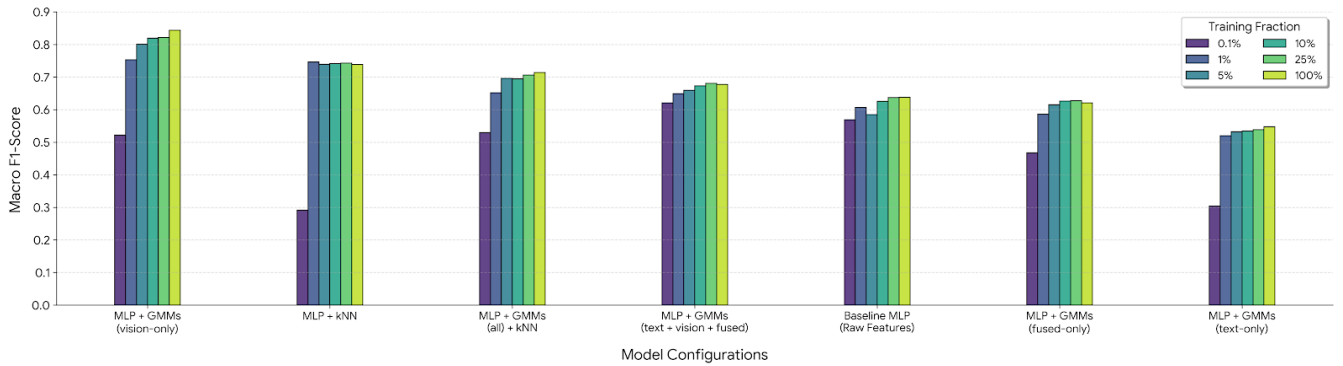


Fig. 3. **Data Scaling and Component Ablation.** Macro F1-Score performance across increasing fractions of training data for different model architectures under ID (LIBERO), partially OOD (LIBERO-PRO), and fully OOD tasks.

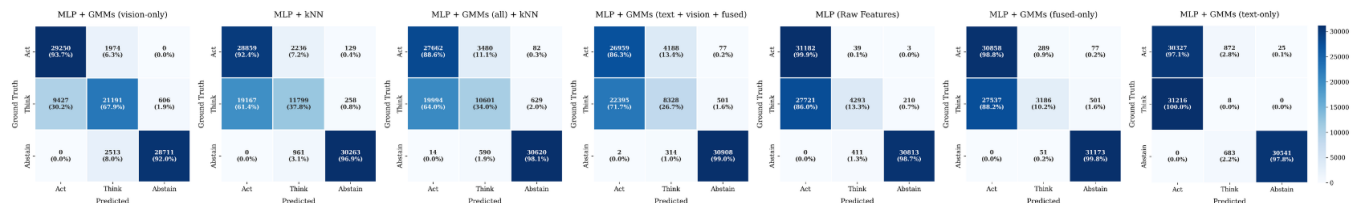


Fig. 4. **Confusion matrices across configurations.** The GMM (vision-only) achieves the best class separation with zero leakage from fully OOD tasks into the "Act" regime. Conversely, the Baseline MLP and multimodal variants show high "Act" bias when evaluating partially OOD tasks.

configurations like the MLP + GMM (all) + kNN ensemble reach an F1-score of 71.41%, they still fail to match the performance of the vision-only variant. The text-only variant performs poorly at 54.76%. We hypothesize that the high-dimensional text embeddings may introduce semantic variability that is not aligned with the spatial cues found in the vision embeddings, thereby weakening the separation of intermediate cases. The text-only and fused configurations appear to struggle specifically with the "Think" path, with the text-only variant failing to identify a single "Think" correctly. These results suggest that including additional modalities could introduce weak correlations that the MLP cannot learn. Without an explicit weighting mechanism, expanding the input space to include additional modalities leads to overfitting on the training set and compromises generalization, especially in partially OOD and OOD tasks. Overall, our study indicates that, for our pipeline, vision-only task complexity estimation via GMMs provides the most reliable signal, and that multimodal fusion is not automatically beneficial and can actually be detrimental under distribution shift.

D. Simulation (RQ3, RQ4)

To quantify the actual usage of our pipeline in simulation environments, we employ our best model from Section IV-C (MLP + GMM vision-only) within two benchmarks: LIBERO and LIBERO-PRO. As defined in Section III-D, all the tasks in LIBERO are in-distribution since the model was fine-tuned on them and exhibits robust performance. These serve as the ground truth for the "Act" path. Contrarily, tasks on LIBERO-PRO (i.e., language, object, swap, task) are perturbed variations of LIBERO (i.e., base), and hence are tasks not completely known to the model but recoverable through

additional reasoning, which is ideal for the "Think" path. Finally, for the OOD tasks involving the "Abstain" policy, we considered tasks that failed with the previous benchmarks. The results presented in Table I provide a comprehensive evaluation of our pipelines' ability to balance operational efficiency with safe execution across various levels of distribution shift. We report examples of simulation rollouts in Figure 5. For the evaluation metrics, we considered Success Rate (SR) with mean and standard deviation across three independent seeds and inference time measured on an NVIDIA RTX Quadro 6000. Safety is quantified by the number of Prevented Failures (PF) as cases in which the Abstain path successfully prevents a subsequent failure. Finally, we show the distribution of Act (A), Think (T), and Abstain (Ab) decisions. For in-distribution tasks, namely the base variants, our pipeline maintains a high success rate by choosing "Act" most of the time. For instance, in the *Goal* and *Object* suites, over 85% of the tasks were executed via the "Act" path, resulting in comparable inference times with respect to the SmolVLA baseline. Crucially, we observe that the "Think" path can boost performance, with a slight increase in success rate. In the *Spatial* and *Long* suites, the "Think" branch recovered several episodes where the baseline failed, yielding a 6.67% improvement for the base variants. As we introduce partial out-of-distribution perturbations, such as language and object variants, the pipeline quickly shifts towards the "Think" and "Abstain" strategies. In the object variant of the *Long* suite, where visual and sequential complexity are significant, the pipeline employs the "Act" path in only 10% of the trials, correctly identifying the higher risk of failure. The main evidence of our framework's safety features is

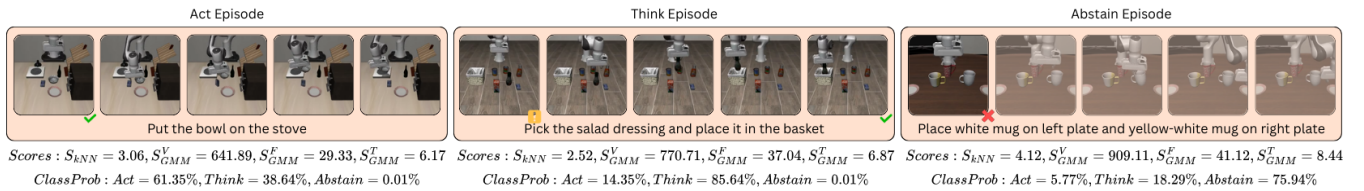


Fig. 5. **Rollout examples on simulation.** Representative episodes from the LIBERO and LIBERO-PRO benchmarks illustrating our adaptive framework. Known tasks are executed with high confidence (left), ambiguous scenarios trigger additional reasoning leading to success later on (center), out-of-distribution tasks are preemptively halted (right).

TABLE I

PERFORMANCE ACROSS LIBERO AND LIBERO_PRO BENCHMARKS.

| Suite | Variant | SmolVLA_LIBERO | | Ours | | | |
|---------|----------|-------------------|----------------------------|-------------------|----|-------------|----------------------------|
| | | SR (%) \uparrow | T_{inf} (s) \downarrow | SR (%) \uparrow | PF | A / T / Ab | T_{inf} (s) \downarrow |
| Goal | base | 83.33 \pm 17.21 | 49.71 | 86.67 \pm 15.34 | 1 | 28 / 1 / 1 | 52.78 |
| | language | 90.00 \pm 11.45 | 52.89 | 90.00 \pm 15.28 | 2 | 26 / 2 / 2 | 53.80 |
| | object | 60.00 \pm 43.51 | 97.73 | 60.00 \pm 44.22 | 10 | 18 / 2 / 10 | 61.42 |
| | swap | 00.0 \pm 0.0 | 163.46 | 00.0 \pm 0.0 | 28 | 0 / 2 / 28 | 4.33 |
| | task | 6.67 \pm 21.08 | 152.24 | 6.67 \pm 21.08 | 27 | 1 / 2 / 27 | 6.12 |
| Object | base | 90.00 \pm 22.51 | 55.43 | 90.00 \pm 21.34 | 1 | 26 / 3 / 1 | 54.82 |
| | language | 90.67 \pm 10.54 | 55.14 | 96.67 \pm 10.54 | 1 | 28 / 1 / 1 | 56.02 |
| | object | 63.33 \pm 39.06 | 91.12 | 66.67 \pm 29.81 | 8 | 19 / 3 / 8 | 69.44 |
| | swap | 00.0 \pm 0.0 | 154.80 | 3.33 \pm 10.54 | 28 | 0 / 2 / 28 | 8.58 |
| | task | 00.0 \pm 0.0 | 156.14 | 00.0 \pm 0.0 | 29 | 0 / 1 / 29 | 3.56 |
| Spatial | base | 73.33 \pm 26.11 | 51.83 | 80.00 \pm 22.11 | 5 | 23 / 2 / 5 | 44.31 |
| | language | 73.33 \pm 26.11 | 69.77 | 76.67 \pm 21.34 | 6 | 22 / 2 / 6 | 60.97 |
| | object | 70.00 \pm 26.44 | 80.35 | 73.33 \pm 24.94 | 7 | 20 / 3 / 7 | 64.34 |
| | swap | 00.0 \pm 0.0 | 157.42 | 00.0 \pm 0.0 | 30 | 0 / 0 / 30 | 3.39 |
| | task | 00.0 \pm 0.0 | 155.92 | 3.33 \pm 10.0 | 28 | 0 / 2 / 28 | 8.79 |
| Long | base | 53.33 \pm 36.96 | 132.24 | 60.00 \pm 29.06 | 10 | 14 / 6 / 10 | 80.91 |
| | language | 43.33 \pm 36.00 | 136.38 | 50.00 \pm 34.16 | 14 | 11 / 5 / 14 | 47.76 |
| | object | 13.33 \pm 26.11 | 149.40 | 16.67 \pm 34.16 | 24 | 3 / 3 / 24 | 21.33 |
| | swap | 00.0 \pm 0.0 | 161.96 | 00.0 \pm 0.0 | 29 | 00 / 1 / 29 | 4.78 |
| | task | 00.0 \pm 0.0 | 162.34 | 00.0 \pm 0.0 | 28 | 00 / 2 / 28 | 5.26 |

found in fully out-of-distribution scenarios, such as *swap* and *task*. Across the different suites, the SmolVLA baseline blindly attempts these tasks, wasting significant time (e.g., more than 150s per episode) before potentially catastrophic failure. In contrast, our adaptive pipeline achieves an almost perfect failure detection, as demonstrated by the high number of prevented failures (PF). For instance, in the task variant of the *Object* suite, the system correctly abstained in 29 out of 30 trials, reducing the average time spent on failed tasks from 153s to only 3s. While the "Think" path results in a negligible computational overhead, the overall average inference time for our pipeline is often significantly lower than the baseline. This result is driven by the "Abstain" path that terminates OOD tasks early, massively preventing failures and saving time. Finally, we observed rare cases of overconfidence in our pipeline, where the system decided for the "Think" path rather than "Abstain" in the presence of a clear OOD shift. While this prevents the system from being perfectly efficient, it suggests a conservative bias toward attempting recovery rather than premature termination. In these cases, the subsequent failure of the "Think" path confirms that the task was fundamentally outside the robot's current capability.

E. Real robot

To evaluate the real-world applicability of our pipeline, we conducted experiments using a SO-ARM 101 on a variety of tabletop manipulation tasks. We fine-tuned SmolVLA on a small set of approximately 100 trajectories recorded with the manipulator. This set established the baseline for the

TABLE II

REAL-ROBOT EVALUATION ON THE SO-ARM 101.

| Model | ID (N = 4) | | Partially OOD (N = 3) | | Fully OOD (N = 3) | | |
|-------|------------|------------|-----------------------|------------|-------------------|----|------------|
| | SR | A / T / Ab | SR | A / T / Ab | SR | PF | A / T / Ab |
| Ours | 4 / 4 | 4 / 0 / 0 | 2 / 3 | 1 / 2 / 0 | 0 / 3 | 0 | 0 / 0 / 3 |

"Act" path. We then evaluated the system across 10 distinct tasks. For the ID tasks, we considered 4 tasks comprising picking, pick&place and block stacking. These tasks utilized the exact object and configurations recorded in the training set. For partially OOD tasks, we used 3 tasks where we introduced variations in terms of object type, color, and positioning. We further challenged the system by providing slightly ambiguous text instructions. Finally, for the OOD tasks, we designed 3 tasks completely outside the model's training distribution, where it would be expected to fail. We report our results in Table II, which mirrors our simulation findings of Section IV-C. For ID tasks, our framework performed flawlessly, successfully executing all four tasks. In the partially OOD tasks, the additional reasoning allowed us to successfully recover two out of three executions. The single failure was due to the system predicting "Act", perhaps being overconfident regarding the complexity of the task. Finally, for fully OOD tasks, the pipeline demonstrates robust performance, correctly triggering "Abstain" for all three tasks and preventing catastrophic failure. These results serve as a test of the pipeline's practical applicability on real robots.

V. CONCLUSIONS

In this work, we introduced an adaptive framework for Vision-Language-Action models, engineered to bridge the gap between performance, operational efficiency, and safe execution. We leveraged an ensemble of density estimators coupled with latent embeddings extracted from the VLM backbone, and we addressed the inherent limitation of standard VLAs when faced with diverse degrees of distribution shift. Our evaluation across the LIBERO and LIBERO-PRO benchmarks, together with real-world experiments on the SO-ARM 101, provided several key insights. Firstly, our pipeline demonstrated a high accuracy in inferring task complexity. In-distribution tasks were efficiently processed via the *Act* path, while partial and fully out-of-distribution shifts triggered additional reasoning or abstention, critically enhancing safety. Secondly, the result of the simulation confirms that the *Think* path effectively increases performance,

recovering successes in ambiguous scenarios where the base model would fail. Finally, our framework never mistakenly abstained from executing in-distribution tasks, improving safety without impacting the overall success rate. Conversely, in fully out-of-distribution scenarios, the system achieved an almost perfect rejection rate, reducing execution time by over 95%. These findings suggest that the future of robust foundation models in robotics lies not only in increasing the capacity of the base models but in developing systems for adaptive inference based on task complexity. Our framework provides a scalable template for deploying VLAs in dynamic and real-world environments where the cost of failure is high and computational resources must be managed cautiously.

VI. LIMITATIONS AND FUTURE WORKS

While our vision-only GMM exhibits convincing performances, there is still a gap in recovering partially OOD tasks that are classified as ID. This is probably due to the transition between *Act*, *Think*, and *Abstain* being managed as a classification problem, and thus creating rigid boundaries at the edges of the distribution shifts. A possible solution for this might be treating the problem as a regression task, where a reinforcement learning policy learns continuous thresholds at runtime using task success as a reward. Furthermore, although our framework is model-agnostic, our experiments are limited to SmolVLA, and we plan to extend evaluation with other VLAs such as π_0 and OpenVLA. Finally, to remove the reliance of our framework on a known in-distribution set, we plan to move towards zero-shot adaptation using text-visual alignment strategies and token uncertainty. We hope that our work will serve as a foundation for more adaptive VLAs, with models that are not just acting but are aware of the inherent complexity of the task.

REFERENCES

- [1] M. Zawalski, W. Chen, K. Pertsch, O. Mees, C. Finn, and S. Levine, "Robotic control via embodied chain-of-thought reasoning," in *Conference on Robot Learning*. PMLR, 2025, pp. 3157–3181.
- [2] Q. Zhao, Y. Lu, M. J. Kim, Z. Fu, Z. Zhang, Y. Wu, Z. Li, Q. Ma, S. Han, C. Finn *et al.*, "Cot-vla: Visual chain-of-thought reasoning for vision-language-action models," in *Proceedings of the Computer Vision and Pattern Recognition Conference*, 2025, pp. 1702–1713.
- [3] Z. Duan, Y. Zhang, S. Geng, G. Liu, J. Boedecker, and C. X. Lu, "Fast ecot: Efficient embodied chain-of-thought via thoughts reuse," *arXiv preprint arXiv:2506.07639*, 2025.
- [4] X. Li, P. Li, L. Qian, M. Liu, D. Wang, J. Liu, B. Kang, X. Ma, X. Wang, D. Guo *et al.*, "What matters in building vision-language-action models for generalist robots," *Nature Machine Intelligence*, pp. 1–15, 2026.
- [5] H. R. Walke, K. Black, T. Z. Zhao, Q. Vuong, C. Zheng, P. Hansen-Estruch, A. W. He, V. Myers, M. J. Kim, M. Du *et al.*, "Bridgedata v2: A dataset for robot learning at scale," in *Conference on Robot Learning*. PMLR, 2023, pp. 1723–1736.
- [6] A. O'Neill, A. Rehman, A. Maddukuri, A. Gupta, A. Padalkar, A. Lee, A. Pooley, A. Gupta, A. Mandlekar, A. Jain *et al.*, "Open x-embodiment: Robotic learning datasets and rt-x models: Open x-embodiment collaboration 0," in *2024 IEEE International Conference on Robotics and Automation (ICRA)*. IEEE, 2024, pp. 6892–6903.
- [7] B. Zitkovich, T. Yu, S. Xu, P. Xu, T. Xiao, F. Xia, J. Wu, P. Wohlhart, S. Welker, A. Wahid *et al.*, "Rt-2: Vision-language-action models transfer web knowledge to robotic control," in *Conference on Robot Learning*. PMLR, 2023, pp. 2165–2183.
- [8] M. J. Kim, K. Pertsch, S. Karamcheti, T. Xiao, A. Balakrishna, S. Nair, R. Raffailov, E. Foster, G. Lam, P. Sanketi *et al.*, "Openvla: An open-source vision-language-action model," *arXiv preprint arXiv:2406.09246*, 2024.
- [9] K. Black, N. Brown, D. Driess, A. Esmail, M. Equi, C. Finn, N. Fusai, L. Groom, K. Hausman, B. Ichter *et al.*, "pi_0: A vision-language-action flow model for general robot control," *arXiv preprint arXiv:2410.24164*, 2024.
- [10] J. Bjorck, F. Castañeda, N. Cherniadev, X. Da, R. Ding, L. Fan, Y. Fang, D. Fox, F. Hu, S. Huang *et al.*, "Gr00t n1: An open foundation model for generalist humanoid robots," *arXiv preprint arXiv:2503.14734*, 2025.
- [11] P. Intelligence, A. Amin, R. Aniceto, A. Balakrishna, K. Black, K. Conley, G. Connors, J. Darpinian, K. Dhabalia, J. DiCarlo *et al.*, " $\pi_{0.6}^*$: a vla that learns from experience," 2025.
- [12] G. Lu, W. Guo, C. Zhang, Y. Zhou, H. Jiang, Z. Gao, Y. Tang, and Z. Wang, "Vla-rl: Towards masterful and general robotic manipulation with scalable reinforcement learning," *arXiv preprint arXiv:2505.18719*, 2025.
- [13] M. Shukor, D. Aubakirova, F. Capuano, P. Kooijmans, S. Palma, A. Zouitine, M. Aractingi, C. Pascal, M. Russi, A. Marafioti, S. Alibert, M. Cord, T. Wolf, and R. Cadene, "Smolvla: A vision-language-action model for affordable and efficient robotics," 2025. [Online]. Available: <https://arxiv.org/abs/2506.01844>
- [14] J. Wen, Y. Zhu, J. Li, M. Zhu, Z. Tang, K. Wu, Z. Xu, N. Liu, R. Cheng, C. Shen *et al.*, "Tinyvla: Towards fast, data-efficient vision-language-action models for robotic manipulation," *IEEE Robotics and Automation Letters*, 2025.
- [15] S. Yang, H. Li, Y. Chen, B. Wang, Y. Tian, T. Wang, H. Wang, F. Zhao, Y. Liao, and J. Pang, "Instructvla: Vision-language-action instruction tuning from understanding to manipulation," *arXiv preprint arXiv:2507.17520*, 2025.
- [16] W. Chen, J. S. Bhatia, C. Glossop, N. Mathihalli, R. Doshi, A. Tang, D. Driess, K. Pertsch, and S. Levine, "Steerable vision-language-action policies for embodied reasoning and hierarchical control," *arXiv preprint arXiv:2602.13193*, 2026.
- [17] F. Lin, R. Nai, Y. Hu, J. You, J. Zhao, and Y. Gao, "Onetovvla: A unified vision-language-action model with adaptive reasoning," *arXiv preprint arXiv:2505.11917*, 2025.
- [18] Q. Gu, Y. Ju, S. Sun, I. Gilitschenski, H. Nishimura, M. Itkina, and F. Shkurti, "Safe: Multitask failure detection for vision-language-action models," in *The Thirty-ninth Annual Conference on Neural Information Processing Systems*, 2025.
- [19] A. Marafioti, O. Zohar, M. Farré, M. Noyan, E. Bakouch, P. Cuenca, C. Zakkā, L. B. Allal, A. Lozhkov, N. Tazi *et al.*, "Smolvlm: Redefining small and efficient multimodal models," *arXiv preprint arXiv:2504.05299*, 2025.
- [20] Y. Lipman, R. T. Chen, H. Ben-Hamu, M. Nickel, and M. Le, "Flow matching for generative modeling," in *The Eleventh International Conference on Learning Representations*, 2023.
- [21] A. Grattafiori, A. Dubey, A. Jauhri, A. Pandey, A. Kadian, A. Al-Dahle, A. Letman, A. Mathur, A. Schelten, A. Vaughan *et al.*, "The llama 3 herd of models," *arXiv preprint arXiv:2407.21783*, 2024.
- [22] D. A. Reynolds *et al.*, "Gaussian mixture models." *Encyclopedia of biometrics*, vol. 741, no. 659-663, p. 3, 2009.
- [23] R. De Maesschalck, D. Jouan-Rimbaud, and D. L. Massart, "The mahalanobis distance," *Chemometrics and intelligent laboratory systems*, vol. 50, no. 1, pp. 1–18, 2000.
- [24] O. Ledoit and M. Wolf, "A well-conditioned estimator for large-dimensional covariance matrices," *Journal of multivariate analysis*, vol. 88, no. 2, pp. 365–411, 2004.
- [25] B. Liu, Y. Zhu, C. Gao, Y. Feng, Q. Liu, Y. Zhu, and P. Stone, "Libero: Benchmarking knowledge transfer for lifelong robot learning," *Advances in Neural Information Processing Systems*, vol. 36, pp. 44 776–44 791, 2023.
- [26] X. Zhou, Y. Xu, G. Tie, Y. Chen, G. Zhang, D. Chu, P. Zhou, and L. Sun, "Libero-pro: Towards robust and fair evaluation of vision-language-action models beyond memorization," *arXiv preprint arXiv:2510.03827*, 2025.
- [27] H. Zhang, M. Cisse, Y. N. Dauphin, and D. Lopez-Paz, "mixup: Beyond empirical risk minimization," in *International Conference on Learning Representations*, 2018.